

RESEARCH

Open Access



Intestinal homeostasis disrupted by Periodontitis exacerbates Alzheimer's Disease in APP/PS1 mice

Xueshen Qian^{1,2}, Xuxin Lin^{1,2}, Weiqiang Hu^{1,2}, Lu Zhang^{1,2}, Wenqian Chen^{1,2}, Shuang Zhang³, Song Ge⁴, Xiongcheng Xu^{1,2*} and Kai Luo^{1,2*}

Abstract

Periodontitis exacerbates Alzheimer's disease (AD) through multiple pathways. Both periodontitis and AD are intricately correlated to intestinal homeostasis, yet there is still a lack of direct evidence regarding whether periodontitis can regulate the progression of AD by modulating intestinal homeostasis. The current study induced experimental periodontitis in AD mice by bilaterally ligating the maxillary second molars with silk and administering *Pg*-LPS injections in APP^{swe}/PS1^{ΔE9} (APP/PS1) mice. Behavioral tests and histological analyses of brain tissue were conducted after 8 weeks. Gut microbiota was analyzed and colon tissue were also evaluated. Then, fecal microbiota from mice with periodontitis was transplanted into antibiotic-treated mice to confirm the effects of periodontitis on AD and the potential mechanism was explored. The results indicated periodontitis exacerbated cognitive impairment and anxious behaviour in APP/PS1 mice, with increased Aβ deposition, microglial overactivation and neuroinflammation in brain. Moreover, the intestinal homeostasis of AD mice was altered by periodontitis, including affecting gut microbiota composition, causing colon inflammation and destroyed intestinal epithelial barrier. Furthermore, AD mice that underwent fecal transplantation from mice with periodontitis exhibited worsened AD progression and disrupted intestinal homeostasis. It also impaired intestinal barrier function, elevated peripheral inflammation, damaged blood-brain barrier (BBB) and caused neuroinflammation and synapses impairment. Taken together, the current study demonstrated that periodontitis could disrupt intestinal homeostasis to exacerbate AD progression potential *via* causing gut microbial dysbiosis, intestinal inflammation and intestinal barrier impairment to induce peripheral inflammation and damage BBB, ultimately leading to neuroinflammation and synapse impairment. It underscores the importance of maintaining both periodontal health and intestinal homeostasis to reduce the risk of AD.

Keywords Periodontitis, Alzheimer's disease, Intestinal homeostasis, Gut microbiota, Inflammation

*Correspondence:

Xiongcheng Xu
xiongchengxu@fjmu.edu.cn

Kai Luo
luokai39@163.com

¹Fujian Key Laboratory of Oral Diseases & Fujian Provincial Engineering Research Center of Oral Biomaterial & Stomatological Key laboratory of Fujian College and University, School and Hospital of Stomatology, Fujian Medical University, Fuzhou, P.R. China

²Institute of Stomatology & Laboratory of Oral Tissue Engineering, School and Hospital of Stomatology, Fujian Medical University, Fuzhou 350002, P.R. China

³Nanjing Stomatological Hospital, Affiliated Hospital of Medical School, Institute of Stomatology, Nanjing University, Nanjing, Jiangsu 210008, P.R. China

⁴School and Hospital of Stomatology, Zunyi Medical University, Zunyi, Guizhou 563003, P.R. China



© The Author(s) 2024. **Open Access** This article is licensed under a Creative Commons Attribution-NonCommercial-NoDerivatives 4.0 International License, which permits any non-commercial use, sharing, distribution and reproduction in any medium or format, as long as you give appropriate credit to the original author(s) and the source, provide a link to the Creative Commons licence, and indicate if you modified the licensed material. You do not have permission under this licence to share adapted material derived from this article or parts of it. The images or other third party material in this article are included in the article's Creative Commons licence, unless indicated otherwise in a credit line to the material. If material is not included in the article's Creative Commons licence and your intended use is not permitted by statutory regulation or exceeds the permitted use, you will need to obtain permission directly from the copyright holder. To view a copy of this licence, visit <http://creativecommons.org/licenses/by-nc-nd/4.0/>.

Introduction

Periodontitis is an inflammatory disease in the supporting tissues of the teeth caused by bacterial plaque biofilm [1]. It can adversely impact several systemic disorders, such as metabolic syndrome [2], cardiovascular diseases [3], diabetes mellitus [4], and cognitive impairment [5, 6].

Alzheimer's disease (AD) is a progressive degenerative disease of the central nervous system. Mounting evidence shows that periodontitis is closely related to the occurrence and progression of AD [7, 8]. Patients with periodontitis have a 1.7-fold risk of developing AD compared to healthy people [9]. *Porphyromonas gingivalis* (Pg) is a primary pathogenic bacterium in periodontitis [10]. Infection with Pg and its toxic component lipopolysaccharide (LPS) has been recognized as an essential risk factor for AD development [11–14]. We previously found that experimental periodontitis could exacerbate AD progression in double-transgenic amyloid precursor protein/presenilin 1 (APP^{sw}/PS1^{ΔE9}; APP/PS1) mice, a model of AD [15]. In a recent study, the administration of Pg, Pg-LPS and gingipains to the tail veins disrupted the permeability of the blood-brain barrier (BBB) and exacerbated cognitive functions in mice [16]. Furthermore, the systemic administration of Pg-LPS was reported to trigger AD-like pathology in mice [17, 18]. These findings indicate that periodontal pathogens and their toxic products can enter the brain and affect AD progression. However, the exact mechanism by which periodontitis affects AD as a local oral inflammation remains unclear.

Intestinal homeostasis is maintained by the dynamic balance between the internal microenvironment and the gut microbiota, along with other components. The gut microbiota consists of trillions of microorganisms that play an important role in dietary energy harvesting. An imbalance in the gut microbiota might worsen colitis and disrupt intestinal homeostasis [19]. Accumulating evidence suggests that disruptions of intestinal homeostasis, including alterations in gut microbiota and its metabolites, exacerbated AD progression, particularly through the “microbiota-gut-brain” axis [20]. Periodontitis could change the composition of the gut microbiota [21]. Previous study has demonstrated intragastric administration of salivary microbiota from periodontitis patients to mice would worsen pathogenesis of AD or anxiety-like behavior [22, 23]. However, the issues of species specificity and the differences in gut microbiota between humans and mice in this study still require further refinement to enhance its persuasiveness. Although an animal study revealed the causal relationship among periodontitis, cognitive decline, and gut microbiota dysbiosis [24], yet there is still a lack of direct evidence regarding whether periodontitis can regulate the progression of AD by modulating intestinal homeostasis.

It is reasonable to hypothesize that periodontitis play a crucial role in the exacerbation of AD *via* orchestrating intestinal homeostasis. The present study tested this hypothesis by a series of experiments. An experimental periodontitis model in AD mice was established to confirm the effects of periodontitis on AD exacerbation. Then fecal microbiota from mice with periodontitis was transplanted into antibiotic-treated AD mice to evaluate whether periodontitis-induced gut microbiota alterations would affect AD progression. Moreover, the potential mechanisms by which periodontitis worsen AD was explored. We believe that this study will reveal a new perspective by which periodontitis affects AD and provide a novel strategy for the prevention and treatment of AD.

Materials and methods

Experimental design

Three-month-old male APP/PS1 mice were purchased from Aniphe Biolaboratory Inc., Jiangsu, China, and raised in a specific pathogen-free environment. After one week of adaptive feeding, all animal operations were performed following the protocol approved by the Animal Ethics Committee of Fujian Medical University (IACUC FJMU 2023-0035). Every effort was made to minimize animal use and suffering. The Animal Welfare and Laboratory protocols were followed according to the ARRIVE Guidelines (Animal Research: Reporting of In Vivo Experiments).

Based on a random sequence generated by a computer, 16 mice were randomly divided into two groups ($n=8$ each): a control group (H-AD) and an periodontitis group (P-AD). Periodontitis was induced by bilateral maxillary second molar silk ligation combined with Pg-LPS injection (InvivoGen, San Diego, CA, USA), as described previously [15]. Control animals of the same age were injected with the same dose of phosphate-buffered saline (PBS) at the exact location. The experimental timeline is shown in Fig. 1a.

Next, 16 mice were randomly allocated into two groups ($n=8$ per group) as follows: control mice that underwent fecal microbiota transplantation (FMT-H-AD) and mice with periodontitis that underwent fecal microbiota transplantation (FMT-P-AD). A mouse model of microbiota depletion was obtained using a large amount of broad-spectrum antibiotics for 2 weeks, as described previously [25]. Subsequently, the fecal microbiota transplantation (FMT) was initiated with normal water consumption. The experimental timeline is shown in Fig. 3a.

Sample collection and preservation

After behavioral testing, the mice were euthanized, and the periodontal tissues (alveolar bone and gingival tissues), blood, colon, cecal contents, and brain (hippocampus and cortex) tissues were collected. The cecal contents

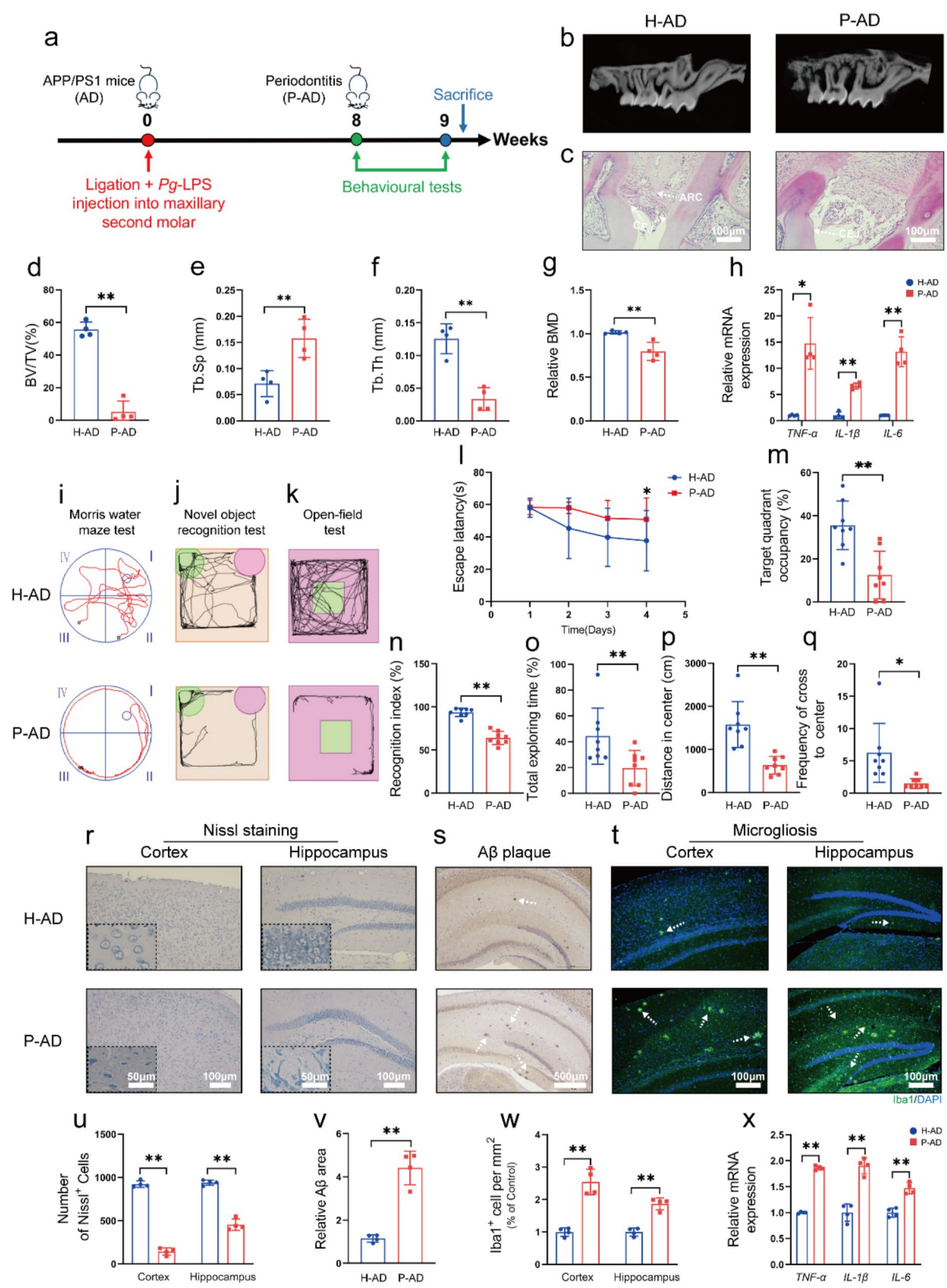


Fig. 1 (See legend on next page.)

(See figure on previous page.)

Fig. 1 Periodontitis exacerbated behavioral disorders and AD-like pathological lesions in the APP/PS1 mice. **(a)** Design of the experiment. **(b)** Mesial-distal micro-CT slices of maxillary molars. **(c)** HE staining of the alveolar bone. **(d–g)** Quantitative analysis of micro-CT data. **(h)** The mRNA levels of *TNF- α* , *IL-1 β* and *IL-6* in gingiva. **(i)** Diagrams showing the swimming paths during the spatial probe period. **(j)** Mice exploring new objects and familiar object path maps. **(k)** The open-field tests included representative tracking images of movement. **(l)** Escape latency of mice to reach the hidden platform. **(m)** Percentage of time utilized by the mice for swimming in the target quadrant. **(n)** New object RI. **(o)** Total time spent exploring new objects. **(p)** Distance of the mice in central area. **(q)** Frequency of the mice of the cross to center. **(r)** Representative images of Nissl staining. **(s)** Representative images of A β immunostaining. **(t)** Representative images of Iba1 immunostaining. **(u)** Quantitative analysis of the number of surviving neurons in cortex and hippocampus. **(v)** Area fractions of relative A β -positive in hippocampus. **(w)** Iba1-positive area fractions in cortex and hippocampus. **(x)** The relative mRNA expression levels of *TNF- α* , *IL-1 β* and *IL-6* in Cortex. * $p < 0.05$, ** $p < 0.01$; ARC: alveolar ridge crest; CEJ: cemento-enamel junction

were collected using a sterile instrument, and 16s ribosomal RNA (16 S rRNA) was sequenced. The proximal colon (about 5 mm) was resected, and the left hemisphere of the brain and alveolar bone were fixed in 4% paraformaldehyde (G1101, Serivicebio, Wuhan, China). The remaining gingival tissues, colon, brain and cortex tissues were immediately frozen in liquid nitrogen and stored at -80°C .

Behavioral assays

Novel object recognition test

A novel object recognition test was performed using a new object recognition device consisting of two detection areas of the same size ($40 \times 40 \times 40$ cm). For the first two days, two similar objects were placed in the corner of the detection area, and the mice were allowed to explore freely for 5 min. On the third day, one of the objects was replaced with a new one of the same size but a different shape, and the time the mice spent exploring the old and new objects were measured. The recognition index (RI) for each mouse was calculated as follows: time spent exploring new objects/time spent exploring new and old objects together $\times 100\%$.

Open-field test

The open-field test device comprised a $40 \times 40 \times 40$ cm plastic partition. Mice were placed in the device along the wall segment with their back against the central region in the same position. Cameras were used to record their movement for 5 min. A tracking software (Tracking Master, Zhongshidichuang, Beijing, China) was used to analyze the activity distance in the central region and the number of times they crossed the central region, and the more time spent in the marginal area, the less time spent in the central area, indicating an increase in anxiety-like behaviors.

Morris water maze test

The water maze device consisted of a white plastic circular pool (radius, 60 cm; height, 50 cm) divided into four quadrants, with a movable platform (10 cm in diameter, 1 cm below the horizontal level) placed in the first quadrant. Directional navigation experiments were conducted during the first 4 days, wherein the time spent searching for an underwater platform after being randomly placed

in one of the four quadrants within 60 s was recorded. If the mice did not successfully find the platform within the specified time, they would be guided onto the platform and allowed to stand there for 20 s, following which the experiment would be ended. The platform exploration experiment was conducted on the fifth day. The platform hidden in the first quadrant of the water was removed, and the number of times the mice crossed the position of the platform and the time they stayed in the target quadrant within 60 s were recorded. These activities were automatically recorded using a behavior analysis system (Tracking Master) for subsequent measurement and analysis.

Micro-computed tomography (CT) and transmission electron microscopy (TEM)

The maxillary tissue was wrapped in plastic and placed in soft foam to prevent it from drying out or displacing during the scan. Micro-CT ($\mu\text{CT}100$; SCANCO Medical, Switzerland) was used to scan the sample, and data measurement using Skyscan software.

Fresh hippocampal tissue was cut into 1 mm^3 sections and fixed in 2.5% glutaraldehyde for 24 h. The sample was fixed in 1% osmic acid for 2 h, dehydrated in gradient acetone, and then embedded in epoxy resin. Semi-thin sections were located, stained with uranium acetate and lead citrate, observed under a TEM (FEI, Tecnai G2 F30, USA), and photographed.

16 S rRNA gene sequencing

The intestinal contents were extracted using the PowerLyzer PowerSoil DNA separation kit (Qiagen, Hilden, Germany) according to the manufacturer's protocol. The extracted DNA was quantified with NanoDrop (Thermo Fisher Scientific, Wilmington, DE, USA) and diluted to $10\text{ ng}/\mu\text{L}$ with DNase and RNase-free water. Universal primers (F: 5'-GTGCCAGCMGCCGCGGTAA-3' and R: 5'-GGACTACHVGGGTWTCTAAT-3') were used to amplify the V3-V4 regions in the bacterial 16 S rRNA. The original sequence was qualitatively filtered using the DADA2 software package. The Greengenes 16 S rRNA reference database (published 13_8) was classified using the q2-feature-classifier. The Wilcoxon rank sum test was performed to determine the significance of α -diversity. The β diversity was analyzed by ANOSIM and visualized

by principal coordinate analysis (PCoA). The sequence data was processed and analyzed using the QIIME 2 software package.

Enzyme-linked immunosorbent assay and Western blot

Colonic tissue, brain tissue and serum were assayed using interleukin (IL)-1 β (ED-20174, LunChangShuoBiotech, Xiamen, China), TNF- α (ED-20852, LunChangShuoBiotech) and LPS (MM-0634M2, MEIMIAN) mouse enzyme-linked immunosorbent assay kits, according to the manufacturers' instructions.

The protein concentration of each sample was determined using the BCA kit (P0009; Beyotime, Shanghai, China). The same amount of protein was denatured at 100 °C for 5 min, separated via sodium dodecyl sulfate-polyacrylamide gel electrophoresis, and transferred onto 0.22- μ m-thick polyvinylidene difluoride membranes (Millipore Corporation, Billerica, MA, USA). The corresponding primary antibodies against ZO-1 (AF5145, Affinity Biosciences), Occludin (DF7504, Affinity Biosciences) and GAPDH (AF7021, Affinity Bioscience) were incubated at 4 °C overnight for detection. Then, the horseradish peroxidase conjugate antibody of the related species was incubated at 37 °C for 1 h. The protein bands were analyzed using the ECL Reagent (MA0186, Meilunbio, Dalian, China) and the Image Lab (Bio-Rad, Hercules, CA, USA) software.

Real-time quantitative polymerase chain reaction (RT-qPCR)

According to the manufacturer's instructions, RNAiso Plus (Takara, Shiga, Japan) was used to extract total mRNA from gum, colon and brain tissue. An ultraviolet spectrophotometer (Q5000; DINGGUOCHANGSHENG Bio Co, Beijing, China) was used to determine the quality and quantity of the RNA, followed by cDNA synthesis. All primers used are listed in the Appendix Table S1.

Hematoxylin and eosin (HE), alcian blue-periodic acid-Schiff (AB-PAS) and nissl staining

The remaining alveolar bone tissue was soaked in 10% ethylene diamine tetraacetic acid (EDTA; 10009618; Sinopharm, Beijing, China) decalcifier (replaced with a new liquid the next day). After 8 weeks, it was gradually dehydrated and embedded in wax blocks. Fresh brain and colon tissue were fixed in 4% paraformaldehyde 48 h later and embedded in the wax block tissue after gradient dehydration. The 5 μ m section stained with HE (G1005, Servicebio, Wuhan, China) was prepared for the observation of periodontal and colon tissue. The colon tissue was histologically scored as previously described [23, 26]. AB-PAS staining was performed according to the manufacturer's instructions (G1049; Servicebio, Wuhan, China) to observe the mucus layer and goblet cells; the

goblet cells were statistically quantified and normalized using the Image J 6.0 software. As described previously [15], serial sections of the left cerebral hemisphere (thickness, 5 μ m) were made. The morphology and quantity of the Nishi bodies in the hippocampus and cerebral cortex were observed by staining with toluidine blue solution (G1436; Solarbio, Beijing, China) at 37 °C for 1 h. Three visual fields were selected to count the neurons in the hippocampus and cortical regions and imaged using a microscope (Eclipse Ci-E, Nikon, Japan).

Immunohistochemistry and immunofluorescence

The brain and intestinal sections (thickness, 5 microns) were soaked in fresh xylene solution twice (10 min each) and diluted with gradient alcohol. The sections were then repaired with citrate antigen at high temperature in a microwave oven for 8 min and incubated with 3% hydrogen peroxide for 30 min to eliminate endogenous peroxidase activity. Sealing was performed with 10% goat serum (MP20008; Yuanye, Shanghai, China) for 30 min, followed by incubation with primary antibodies against A β ₁₋₄₂ (ab201061; Abcam), Iba1 (DF6442; Affinity Biosciences), ZO-1 (AF5145; Affinity Biosciences), Occludin (DF7504; Affinity Biosciences) at 4 °C overnight. After three washes with PBS on the second day, the sections were incubated with the corresponding secondary antibody at 37 °C for 1 h. The immunohistochemical sections were colored with DAB (DAB-0031; MXB, Fuzhou, China) under a microscope and imaged using a microscope (Eclipse Ci-E, Nikon, Japan). Immunofluorescence was observed under a fluorescence microscope (IX71; Olympus, Japan) after incubation with DAPI solution (28718-90-3; Solarbio, Beijing, China) for 10 min in the dark. The Image J system was used to record the average optical density and fluorescence intensity.

Statistical analyses

All experimental data were analyzed using SPSS 26.0 statistical software and are expressed as mean \pm standard deviation. Analysis of variance (ANOVA) of repeated measurement data was used to analyze the Morris water maze experimental data, and the Kolmogorov-Smirnov test was used to determine whether the data followed a normal distribution. A one-way ANOVA was performed if normal distribution was observed, followed by a post-hoc test. The Kruskal-Wallis or Mann-Whitney U tests were used if the distribution was abnormal. $p < 0.05$ was considered statistically significant. GraphPad Prism 9 software was used to plot the experimental data statistically.

Results

Periodontitis exacerbated behavioral disorders and AD-like pathological lesions in the APP/PS1 mice

Significant alveolar bone loss was detected by micro-CT in the P-AD group (Fig. 1b), which was characterized by considerable bone loss in the maxillary second molar region. Obvious reduction in trabecular bone volume fraction, trabecular separation, trabecular thickness, and relative bone mass density was observed compared to the H-AD group (Fig. 1d–g). Additionally, alveolar bone resorption, breakdown of collagen fibers and infiltration of inflammatory cells were observed in the P-AD group (Fig. 1c). Furthermore, the mRNA expression levels of *TNF- α* , *IL-1 β* and *IL-6* were notably enhanced in the gingival tissues (Fig. 1h). These results showed that the periodontitis model in AD mice was established successfully.

Behavioral tests were performed after 8 weeks of the establishment of periodontitis. In the Morris water maze test, the mice's escape latency was gradually shortened after 4 days of directional navigation training. On the 4th day, the escape latency was significantly decreased in the H-AD group compared to that in the P-AD group (Fig. 1l). After the platform was removed on the 5th day, the mice in the P-AD group spent significantly less time in the target quadrant (Fig. 1m); their search pattern indicated that they could not recall the platform's location even after training (Fig. 1i). During the target recognition test, the P-AD mice exhibited a lower RI and total exploration time than the H-AD mice (Fig. 1j, n and o), indicating that the P-AD mice had a lower level of curiosity and willingness to explore new objects and impaired spatial memory. In the open-field experiment, the P-AD mice significantly reduced the distance and frequency across the central region compared to the H-AD mice, indicating increased stress and anxiety (Fig. 1k, p and q).

We explored the morphology and number of neurons in the hippocampus and cortical regions to observe the AD-like pathological changes in the brains of APP/PS1 mice induced by periodontitis. Nissl staining showed that the number of neurons was significantly reduced in the P-AD group, and the morphological structure was severely damaged (Fig. 1r and u). A β_{1-42} (Fig. 1s and v) immunohistochemical staining demonstrated that the brains of mice in the P-AD group had more A β deposition, thus indicating that early infection with periodontitis could worsen the development of AD-like lesions in APP/PS1 mice. The expression levels of *TNF- α* , *IL-1 β* and *IL-6* were sharply increased in cortex of the mice (Fig. 1x). Similarly, the overactivated microglia were stained with ionized calcium-binding adaptor molecule 1 (Iba1) in the brains of the P-AD mice (Fig. 1t and w). Overall, these results revealed that periodontitis aggravated behavioral disorders and the pathological changes

of AD in APP/PS1 mice, like neuronal loss, A β deposition and neuroinflammation.

Periodontitis led to disruptions of intestinal homeostasis in the APP/PS1 mice

The histological analyses of colon tissue were conducted to assess the effect of periodontitis on the intestinal homeostasis. HE staining showed colonic mucosal inflammation in P-AD group (including inflammatory cell infiltration, tissue hydrolysis and crypt structure damage) was significantly higher than in the H-AD group (Fig. 2a and e). AB-PAS staining showed a significant reduction in colonic goblet cells in the P-AD group, indicating damage to the mucous layer of the intestine (Fig. 2b and f). ZO-1 and Occludin are tight junction proteins that are essential in maintaining the intestine barrier [27]. The expression levels of ZO-1 and Occludin were significantly down-regulated in the colons of mice in the P-AD group compared to those in the H-AD group (Fig. 2c–d and g–h). The expression of inflammation-related genes (such as *TNF- α* , *IL-1 β* , *IL-6* and *IL-10*) between H-AD and P-AD groups were similar (Fig. 2i).

The compositions of gut microbiota between the P-AD and H-AD groups were analyzed to evaluate the effect of periodontal infection during AD progression. Although α diversity analyses of 16 S rRNA sequencing results indicated there was no significant difference in the P-AD group with the H-AD group (Fig. 2k), the Venn diagram of bacteria and β diversity conducted using the PCoA based on Bray Curtis dissimilarity metrics revealed significant differences in the microbial composition and structures between the two groups (Fig. 2j and i). Specifically, at the phylum level, the relative abundance of *Firmicutes* decreased while that of *Bacteroidetes* increased (Fig. 2m). It is worth mentioning that the relative abundance of *Proteobacteria* in the P-AD group was increased. Previous research indicated that an increase in *Proteobacteria* is a sign of more pronounced gut microbiota disruption [28]. Notably, significant changes in the genus level were observed after periodontal infection. Harmful intestinal bacteria, such as *Ruminococcus* and *Sutterella* were increased in the P-AD group, whereas beneficial bacteria, including *Lactobacillus* and *Allobaculum* were decreased, compared to those in the H-AD group (Fig. 2n). Conduct a Spearman correlation analysis between gut microbiota and parameters related to periodontitis to identify specific gut microbial communities that may be altered under the influence of periodontitis. *Lachnospiraceae clostridium* and *Sutterella* were positively correlated with most periodontitis phenotypes, while *Anaerostipes* were negatively correlated with the periodontitis-related parameters (Fig. 2o). The above results suggested that periodontitis led to disruptions of intestinal homeostasis in the APP/PS1 mice.

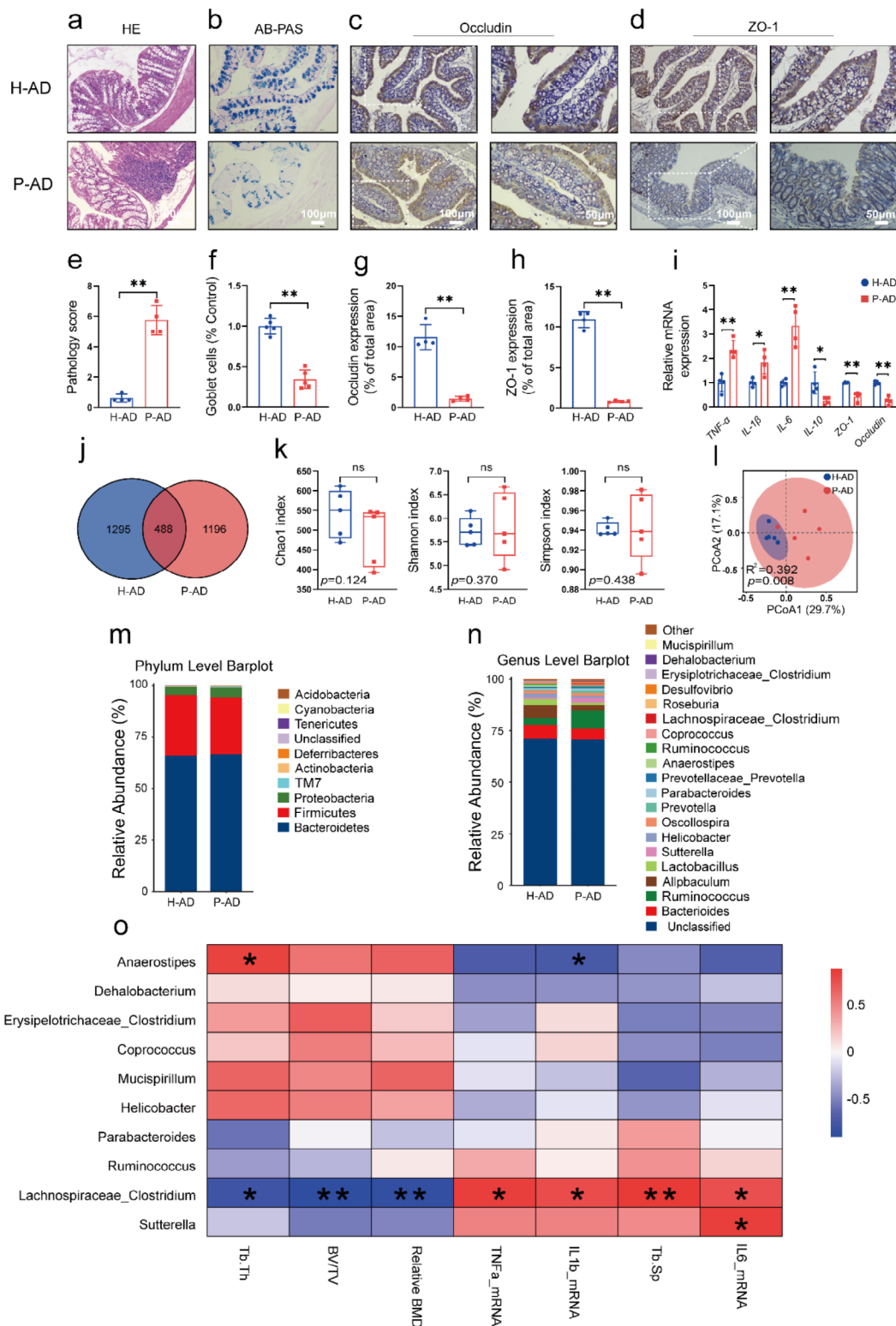


Fig. 2 Periodontitis led to disruptions of intestinal homeostasis in the APP/PS1 mice. **(a)** HE staining of colon. **(b)** AB-PAS staining. **(c)** Representative images of ZO-1 immunostaining. **(d)** Representative images of Occludin immunostaining. **(e)** Histological score of the colon. **(f)** Quantitative analysis of Goblet cells. **(g-h)** Quantitative analysis of ZO-1 and Occludin expression. **(i)** The relative mRNA expression levels of *TNF- α* , *IL-6*, *IL-1 β* , *IL-10*, *ZO-1* and *Occludin* in the colon. **(j)** Venn diagram showing the difference in ASV between the H-AD and P-AD groups. **(k)** The diversity of Chao1 index, Shannon index and Simpson index. **(l)** PCoA analysis. **(m-n)** Periodontitis changes the overall composition of the gut microbiota in phylum **(m)** and genus levels **(n)**. **(o)** Spearman correlation analysis between gut microbiota and parameters related to periodontitis. * $p < 0.05$, ** $p < 0.01$, ns: not significant

Transplantation of periodontitis-altered gut microbiota worsened behavioral disorders and AD-like pathology in AD mice

The effect of gut microbiota disturbances by periodontal infection on AD-like changes was verified by transplanting fecal microbiota from the H-AD and P-AD groups into antibiotic-treated APP/PS1 mice (FMT) *via* gavage (Fig. 3a). No obvious periodontal destruction could be observed in both FMT-H-AD and FMT-P-AD groups (Fig. S1). The Morris water maze test results demonstrated that the escape latency of the FMT-P-AD mice was significantly higher than that of the FMT-H-AD mice (Fig. 3b, e). Additionally, the percentage of stay time in the target quadrant was significantly reduced in the FMT-P-AD group (Fig. 3f). Behavior results indicated that the transplantation of fecal bacteria aggravated the memory impairment of the FMT-P-AD mice. Furthermore, the FMT-P-AD mice showed a lower desire to explore and decreased curiosity in the new object recognition test, suggesting impaired spatial memory ability (Fig. 3c, g and h). Finally, in the open-field test, the FMT-P-AD mice showed more stress and depression than the FMT-H-AD group (Fig. 3d, i and j). These behavioral results revealed that FMT-P-AD mice exerted an exacerbating behavioral disorders similar to that in the P-AD group after fecal transplantation.

Regarding the AD-like pathological changes, a greater degree of neuronal structure disorganization was observed in the hippocampal DG region and the cortical areas in FMT-P-AD mice, accompanied by evident cellular damage and a significant reduction in the number of surviving neurons (Fig. 3k and n). Similarly, more A β deposition was observed in the brain of FMT-P-AD mice after immunohistochemical staining (Fig. 3l and o). Furthermore, FMT intensified the activation of the microglia in the hippocampus and cortical regions of the FMT-P-AD mice (Fig. 3m and p). Consistent with the results in the P-AD group, after FMT, brain inflammation genes in the FMT-P-AD group were significantly increased (Fig. 3q). These findings showed that transplantation of the gut microbiota from mice with periodontitis to antibiotic-treated mice could partially alter the AD-like pathological changes in the brain.

Transplantation of periodontitis-altered gut microbiota into AD mice caused disruptions of intestinal homeostasis

The intestinal epithelial barrier of antibiotic-treated mice after fecal transplantation was evaluated in this study. Histological results showed that the colons of mice in the FMT-P-AD group had significant lymphocyte infiltration and a reduced number of goblet cells (Fig. 4a, b, e and f). The expression levels of Occludin and ZO-1 were significantly decreased in the FMT-P-AD group (Fig. 4c, d, g, h). In addition, the relative mRNA expression of *TNF- α* ,

IL-1 β , *IL-6*, *IL-10*, *ZO-1* and *Occludin* in FMT-P-AD group showed similar results with P-AD group (Fig. 4i).

The gut microbiota compositions of FMT-H-AD and FMT-P-AD groups were analyzed. The Venn diagram was constructed to describe the similarities in bacterial populations among different samples. The lowest and highest numbers of unique sequences were detected in the FMT-P-AD (1515) and FMT-H-AD (1730) groups, respectively (Fig. 4j); only 565 consensus sequences were detected between the two groups. The α diversity analysis results indicated the gut microbiota in the FMT-P-AD and FMT-H-AD group were similar (Fig. 4k). PCoA based on the Bray Curtis distance metrics with β diversity showed significant differences in microbiota composition in the FMT-P-AD group compared to that in the FMT-H-AD group (Fig. 4j and l). At the phylum level, the relative abundance of *Bacteroidetes* in the FMT-P-AD group decreased. But the ratio of *Bacteroidetes* to *Firmicutes* and the abundance of *Proteobacteria* increased in the FMT-P-AD group (Fig. 4m). In the current study, we observed a decrease in beneficial bacteria, like *Lactobacillus* and *Anaerostipes*. While the harmful bacteria, such as *Oscillospira*, *Erysipelotrichaceae clostridium* and *Lachnospiraceae clostridium*, were increased at the genus level (Fig. 4n). These data suggested that transplantation of periodontitis-altered gut microbiota induced intestinal homeostasis disruption in AD mice.

The potential mechanisms of disruptions of intestinal homeostasis on exacerbation of AD by periodontitis

A series experiments were conducted to explore the potential mechanism of intestinal homeostasis disrupted by periodontitis on AD. Significant increased levels of LPS, TNF- α and IL-6 could be observed in the colon of FMT-P-AD group (Fig. 5c, d). In addition, colon macrophages were activated in FMT-P-AD group (Fig. 5a-b). Blood levels of LPS, TNF- α and IL-6 were also significantly increased in FMT-P-AD group (Fig. 5e, f). The breakdown of the BBB is reported to be crucial in the development of AD [29, 30]. Under normal circumstances, the paracellular space is tightly connected and sealed to maintain the integrity and function of the barrier [30, 31]. In the current study, we evaluated the integrity of the BBB to determine whether neuroinflammation and increased amyloid levels in the brain were related to BBB leakage. Western blot analysis showed that the expression levels of ZO-1 and Occludin in Cortex in the FMT-P-AD group were significantly decreased compared to those in the FMT-H-AD group (Fig. 5h-i). As shown in Fig. 5g, the ultrastructure of the BBB could be observed under TEM, which indicated astrocytic end-feet embracing the capillaries were swollen in the FMT-P-AD mice. In contrast, the surfaces of the vascular endothelial cells and basement membranes in the FMT-H-AD mice were

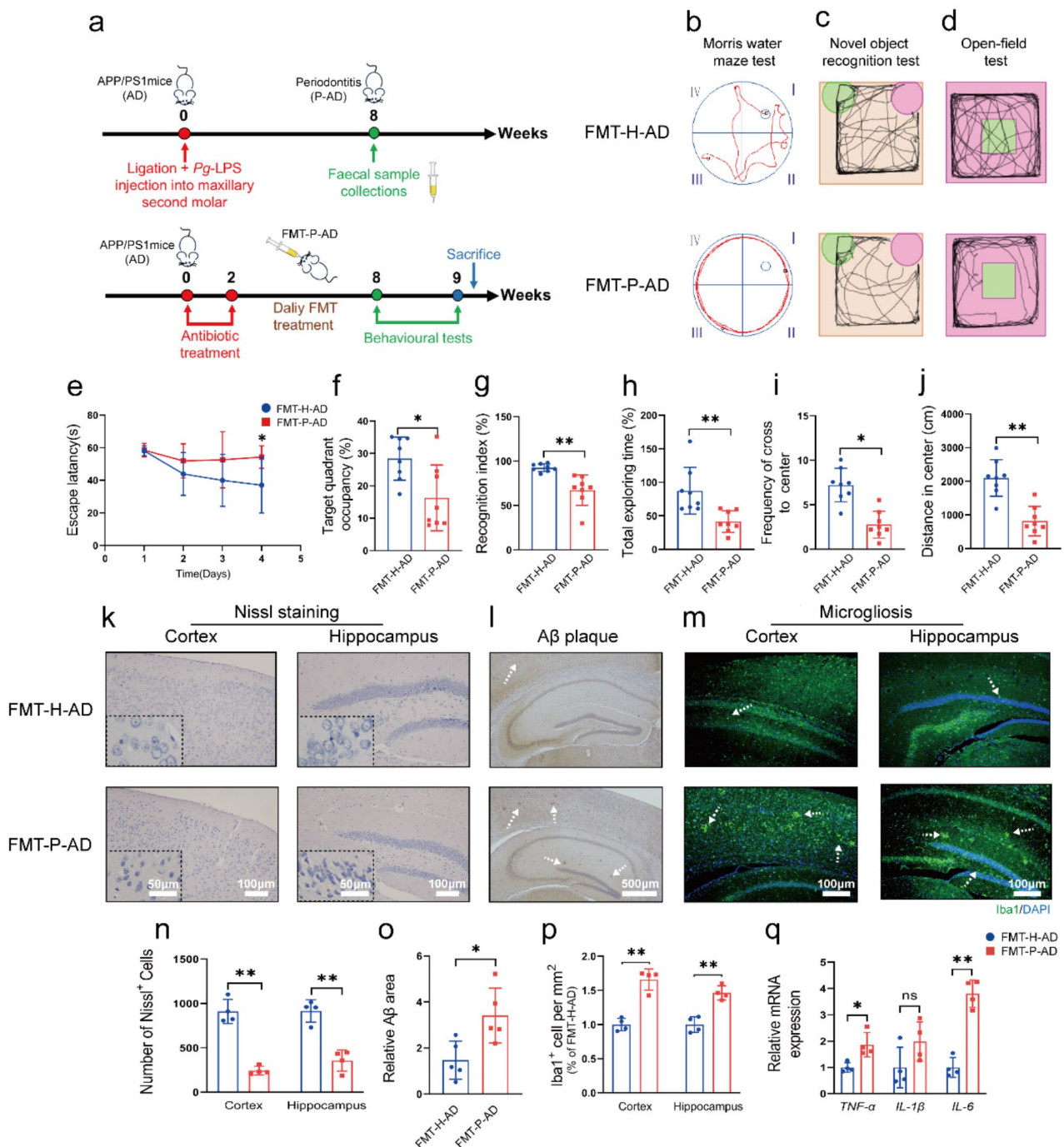


Fig. 3 Transplantation of periodontitis-altered gut microbiota worsened behavioral disorders and AD-like pathology in AD mice. **(a)** Design of the experiment. **(b)** Diagrams showing the swimming paths during the spatial probe period. **(c)** Mice explore new objects and familiar object path maps. **(d)** The open-field test included representative tracking images of movement. **(e)** Escape latency of mice to reach the hidden platform. **(f)** Percentage of time utilized by the mice for swimming in the target quadrant. **(g)** New object RI. **(h)** Total time spent exploring new objects. **(i)** Frequency of the number of times the mice cross to center. **(j)** Distance of the mice in central area. **(k)** Representative images of Nissl staining. **(l)** Representative images of A β immunostaining. **(m)** Representative images of Iba1 immunofluorescence staining. **(n)** Quantitative analysis of the number of surviving neurons in cortex and hippocampus. **(o)** Fractions of A β -positive area. **(p)** Quantitative analysis of the area fraction in the cortex and hippocampus. **(q)** The relative mRNA expression levels of *TNF- α* , *IL-1 β* and *IL-6* in the Cortex. * $p < 0.05$, ** $p < 0.01$

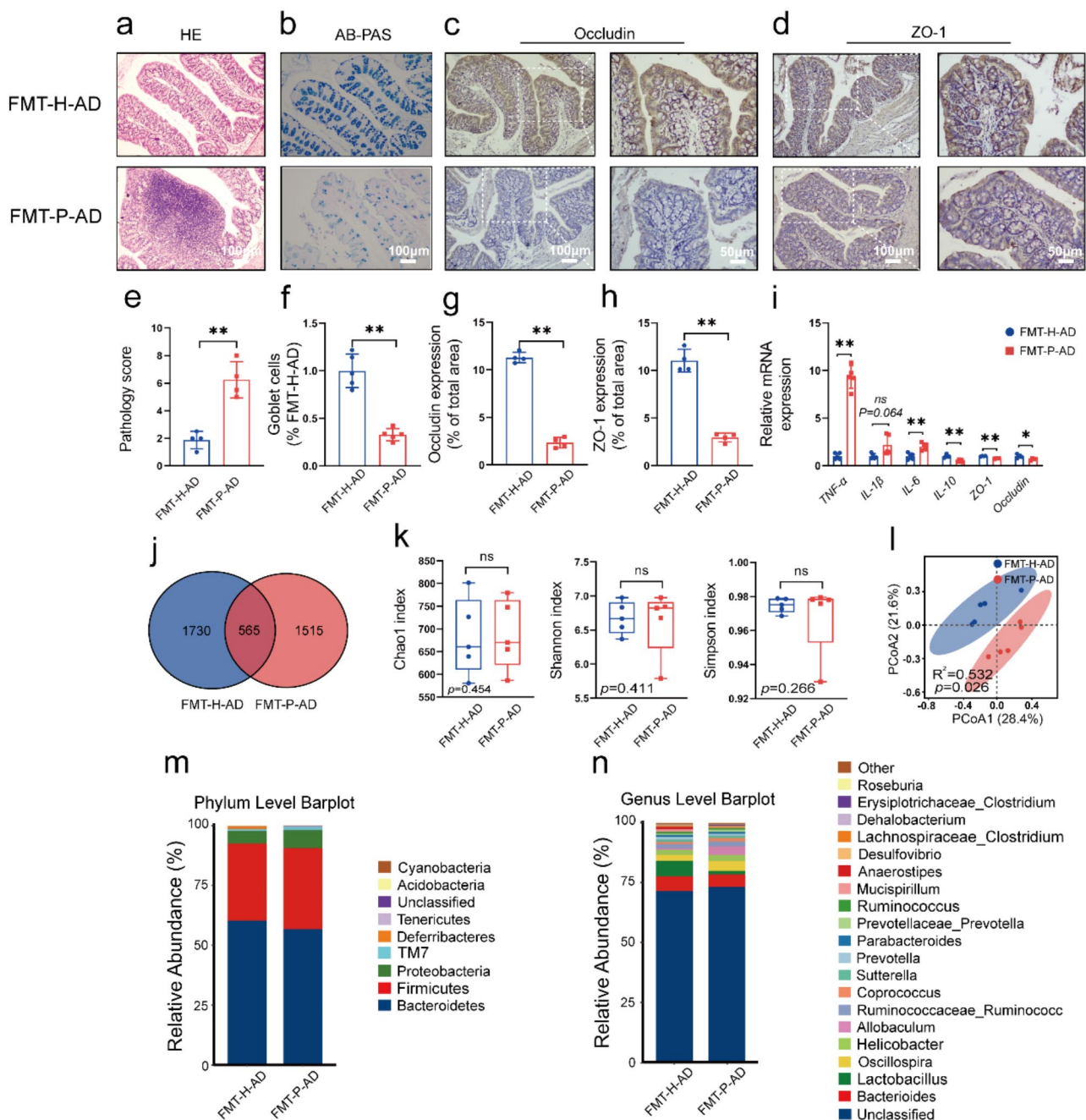


Fig. 4 Transplantation of periodontitis-altered gut microbiota into AD mice caused disruptions of intestinal homeostasis. **(a)** HE staining of colon. **(b)** AB-PAS staining. **(c)** Representative images of ZO-1 immunostaining. **(d)** Representative images of Occludin immunostaining. **(e)** Histologic score of the colon. **(f)** Quantitative analysis of Goblet cells. **(g)** Quantitative analysis of Goblet cells. **(h)** Quantitative analysis of ZO-1 and Occludin expression. **(i)** The relative mRNA expression of *TNF-α*, *IL-1β*, *IL-6*, *IL-10*, *ZO-1* and *Occludin* in the colon. **(j)** Venn diagram showing the difference in ASV between the FMT-H-AD and FMT-P-AD groups. **(k)** The α diversity of Chao1 index, Shannon index and Simpson index. **(l)** PCoA analysis. **(m-n)** Transplantation of periodontitis altered the overall composition of the gut microbiota at phylum (**m**) and genus (**n**) levels. * $p < 0.05$, ** $p < 0.01$ versus the FMT-H-AD group

smooth and complete; the layer was transparent, and no edema was observed in the foot processes of the astrocytes. ELISA showed that LPS, $\text{TNF-}\alpha$ and $\text{IL-1}\beta$ levels were significantly increased in the hippocampal tissues of the FMT-P-AD group (Fig. 5j-k). In addition, the number of presynaptic vesicles was decreased, with some

synaptic clefts appearing blurred, and a reduction in the dense structures of the postsynaptic membrane (Fig. 5l). Immunofluorescent staining demonstrated that FMT-P-AD mice exhibited a greater accumulation of microglia surrounding A β deposits in both the hippocampus and cortex, with a notable increase in the size of these glial

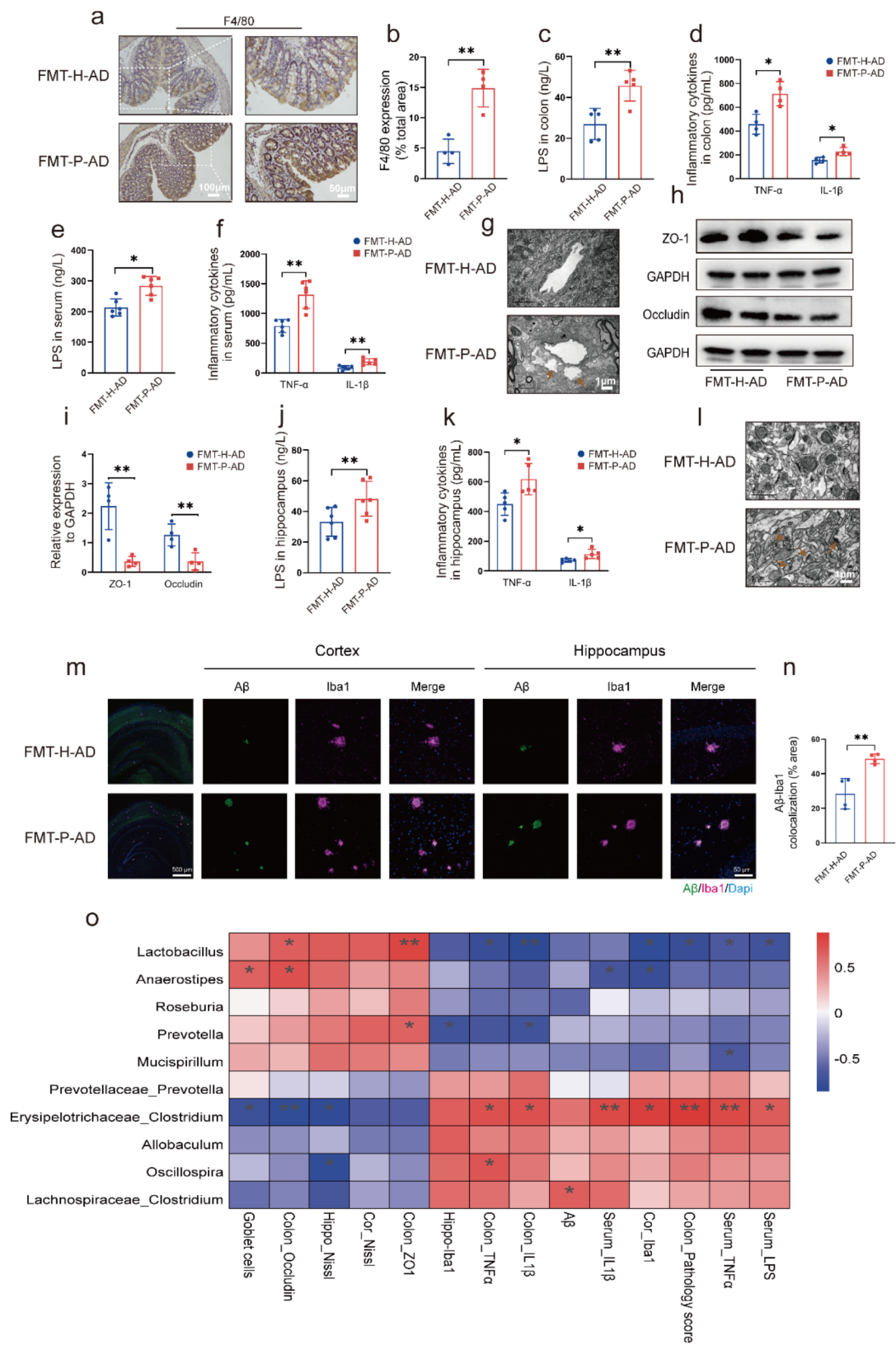


Fig. 5 (See legend on next page.)

(See figure on previous page.)

Fig. 5 The potential mechanisms of disruptions of intestinal homeostasis on exacerbation of AD by periodontitis. **(a)** Representative images of F4/80 immunostaining. **(b)** Quantification of F4/80-positive area fractions in the colon. **(c–d)** The levels of LPS, TNF- α and IL-1 β in colon. **(e–f)** The levels of LPS, TNF- α and IL-1 β in peripheral blood. **(g)** Representative images of TEM with BBB. The arrow shows the astrocytic end-feet swelling. **(h–i)** Western blot and quantitative analysis of ZO-1 and Occludin in Cortex. **(j–k)** The levels of LPS, TNF- α and IL-1 β in hippocampus. **(l)** Representative images of TEM with synapses. The arrow shows blurring of synaptic cleft structure. **(m–n)** Immunofluorescence localization and quantification of Iba1 (green) and A β (magenta) in cortex and hippocampus. **(o)** Spearman correlation analysis with intestinal lesions, brain AD-like lesions, peripheral blood inflammation and gut microbiota. * $p < 0.05$, ** $p < 0.01$

cells, compared to FMT-H-AD mice. This may hint that the increase of A β promoted the activation and phagocytosis of microglia (Fig. 5m–n).

Spearman's correlation analysis was performed on the correlation parameters between the gut microbiota and brain AD-like lesions, pathological manifestations of peripheral blood inflammation and intestinal lesions (Fig. 5m). *Erysipelotrichaceae_Clostridium* in the cecum of FMT-P-AD mice was significantly positively correlated with pathological manifestations of colon, peripheral inflammation and AD-like lesions in the brain. However, *Lactobacillus* and *Anaerostipes* in the cecum were negatively correlated. These data suggested that the increase of harmful bacteria after FMT might exacerbate intestinal pathological injury, peripheral inflammation and AD-like changes in the brain. Taken together, we speculated that periodontitis exacerbated AD progression potential *via* causing gut microbial dysbiosis, intestinal inflammation and intestinal barrier impairment to induce peripheral inflammation and damage BBB, ultimately leading to neuroinflammation and synapse impairment.

Discussion

Growing evidence indicates periodontitis is a risk factor for AD [7, 18, 32, 33]. Previous studies suggest both periodontitis and AD are intricately linked to intestinal homeostasis [34–36], yet there is still a lack of direct evidence regarding whether periodontitis could regulate AD progression by modulating intestinal homeostasis. The current study demonstrated that periodontitis could disrupt intestinal homeostasis to exacerbate AD progression potential *via* causing gut microbial dysbiosis, intestinal inflammation and intestinal barrier impairment to induce peripheral inflammation and damage BBB, ultimately leading to neuroinflammation and synapse impairment. As far as we know, this is the only direct evidence currently available show that periodontitis might influence AD lesions by its local inflammatory effects to disrupt intestinal homeostasis.

Animal models, primarily transgenic mice engineered to express human genes, have been used as predominant AD experimental models [37]. The APP/PS1 mouse, a classic AD mouse model, showed no difference in response from wild-type mice at 3 months of age; additionally, they develop spatial learning and memory impairments at 6 months old and amyloid plaque deposits, a pathology that is exacerbated with advancing age, at

9 months old [38–40]. In the current study, 3-month-old APP/PS1 mice were selected to simulate the early stages of human AD [38, 39]. Periodontitis is a chronic inflammatory disease affecting the periodontal supporting tissues, caused by dental plaque. In our previous study, we successfully established an experimental periodontitis model in mice by ligating the maxillary second molar with silk combined with *Pg*-LPS injection [15]. This study established a periodontitis model in AD mice using the same method, and found that AD mice with periodontitis exhibited worsened cognitive impairment and AD-like pathological changes. It indicated silk ligation combined with local *Pg*-LPS injection can further simulate the oral microenvironment of teeth affected by periodontitis and the inflammatory microenvironment within periodontal supporting tissues, thus exacerbating AD-like lesion.

The progression of AD has been reported to be exacerbated by periodontitis, either by inducing peripheral inflammation or allowing periodontal pathogens and their toxic products to reach the brain through the bloodstream [41, 42]. Recent studies have demonstrated that dysregulation of intestinal homeostasis is closely related to the progression of AD [20, 43]. An imbalance in the gut microbiota may destroy the integrity of the intestinal barrier and increase its permeability, leading to intestinal leakage [44], which further affect neural health, thereby influencing the onset and progression of AD [45]. Previous studies have shown that the intestinal barrier integrity was compromised in mice following the intra-gastric administration of saliva from individuals with periodontitis [23, 46], intragastric delivery of periodontal pathogens [47–49], systemic exposure to *Pg*-LPS [50] and induction of periodontitis *via* silk ligature [51, 52]. The present study also found that AD mice with periodontitis exhibited significant inflammatory infiltration in the colon tissue, disruption of the intestinal mucus layer and marked alterations in the gut microbiota.

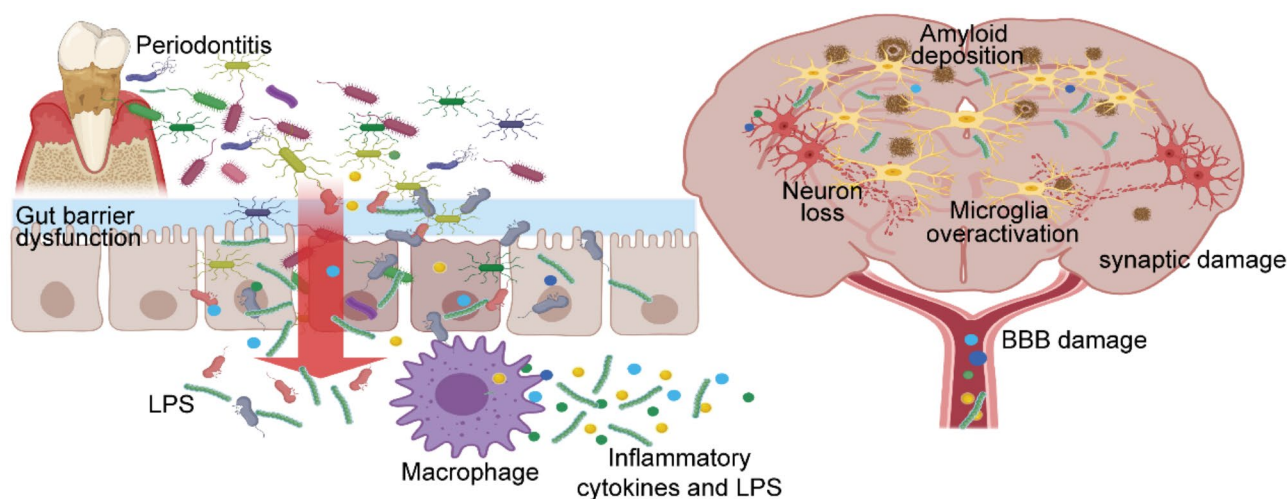
Previous studies have found that the composition and abundance of gut microbiota in patients with AD or periodontitis differ from those in healthy individuals [53–56]. The present study indicated a decrease in *Firmicutes* and an increase in *Bacteroidetes* at the phylum level in AD mice with periodontitis, consistent with observations in AD patients [57]. Specifically, periodontitis increased the relative abundance of *Ruminococcus* and decreased *Lactobacillus* and *Allobaculum* in the gut microbiota at the genus level. Dysregulation of *Ruminococcus* could act as

a predictive marker for rapidly progressive mild cognitive impairment [58, 59]. Both *Lactobacillus* and *Allobaculum* play vital roles in intestinal immunity. *Lactobacillus* can stimulate the maturation and activation of dendritic cells and affect the function and activity of immune cells [60]. *Allobaculum* is physiologically capable of using carbohydrates to produce butyric acid. It up-regulates the abundance of tight-linking proteins to maintain the intestinal barrier and can prevent dendritic cell activation and T cell expansion, readjusting the immune environment of mesenteric lymph nodes [61, 62]. The results of the current study are consistent with those of previous studies, which have demonstrated that periodontitis can induce alterations in the composition of the gut microbiota [51, 63]. Furthermore, *Lachnospiraceae clostridium* and *Sutterella* were positively correlated with parameters related to periodontitis (Fig. 2). However, beneficial bacteria such as *Anaerostipes* were negatively correlated. Combined with the cognitive behavior and AD-like pathological changes in AD mice with periodontitis, we speculate that intestinal homeostasis disruption may be one of the factors contributing to the exacerbation of AD by periodontitis.

To further clarify the role of intestinal homeostasis in the exacerbation of periodontitis during AD progression, microorganisms from the fecal of AD mice with periodontitis were transplanted to antibiotic-treated mice, as described previously [64, 65]. The transplantation of fecal from mice with periodontitis didn't affect the periodontal health, but altered the gut microbiota, disrupted intestinal homeostasis and exacerbated the progression of AD. Spearman's correlation analysis showed that probiotics, such as *Lactobacillus* and *Anaerostipes*, were negatively correlated, whereas *Erysipelotrichaceae clostridium* was positively correlated with AD-like pathological changes

in the brains of AD mice following fecal transplantation from mice with periodontitis. Notably, probiotics like *Lactobacillus* and *Anaerostipes* were declined in AD mice with periodontitis or following fecal transplantation from mice with periodontitis, suggesting that these bacteria might play a key role in the impact of periodontitis on AD progression. Multiple reports have shown the neuroprotective effects of *Lactobacillus* against AD [66, 67]. *Anaerostipes* was used as a probiotic to maintain body health because they can ferment xylitol and produce butyrate which were associated with mild cognitive impairment [68–70]. These findings suggested that the increase of harmful bacteria after fecal bacteria transplantation might exacerbate AD-like pathological changes in APP/PS1 mice, *Lactobacillus* and *Anaerostipes* have the potential to be used as probiotics to slow the progression of AD (See Scheme 1).

The gut-brain crosstalk plays a principal role in the occurrence and progression of AD [71]. Disruptions of intestinal homeostasis, including imbalance of the gut microbiota, affects the pathogenesis and progression of AD *via* the gut-brain axis [72]. In the present study, our results showed that the colon tissue existed damaged intestinal epithelial barrier, the aggregation of macrophages and higher levels of LPS and pro-inflammatory cytokines in the colon tissues of AD mice following transplantation of periodontitis-altered gut microbiota. In particular, the concentrations of LPS and pro-inflammatory cytokines in the serum were also significantly increased in the AD mice following transplantation of periodontitis-altered gut microbiota. These findings implied that intestinal homeostasis was disrupted by periodontitis, and the breakdown of the intestinal epithelial barrier might promote the translocation of enterogenic endotoxin LPS and inflammatory factors, thus



Scheme 1 A schematic illustrates how periodontitis exacerbated AD progression potential *via* causing gut microbial dysbiosis, intestinal inflammation and intestinal barrier impairment to induce peripheral inflammation and damage BBB, ultimately causing neuroinflammation and synapse impairment

inducing peripheral inflammation. Based on current researches [73–75], we speculated that periodontitis in this study may change the gut microbiota composition through different pathways, including oral and hematogenous routes. Oral pathogens and their metabolites caused by periodontitis can enter the gut during swallowing and feeding, subsequently leading to changes in gut microbiota composition. Inflammatory factors and toxic products generated during the inflammatory process of periodontitis can enter the bloodstream, inducing a systemic inflammatory response that disrupts intestinal homeostasis and further alters gut microbiota composition.

The decrease in the expression of the tight junctional proteins and the edema of the astrocytic end-feet observed in the brain tissue ultrastructure indicated that the BBB was damaged to a certain extent in the AD mice following transplantation of periodontitis-altered gut microbiota. The pro-inflammatory factors and LPS in the bloodstream may cross the BBB and reach the brain, then worsen neuroinflammation, overactivation of the microglia and A β deposition and impair synapses. Interestingly, we also found that FMT-P-AD mice exhibited a higher density of activated microglia surrounding A β plaques. Considering the exacerbation of AD-like pathology in FMT-P-AD mice, this suggested that excessive phagocytosis of pathological proteins may impair the phagocytic capacity of microglia, triggering neuroinflammation and leading to neurodegeneration [76]. Taken together, we speculated that periodontitis exacerbated AD progression potential *via* causing gut microbial dysbiosis, intestinal inflammation and intestinal barrier impairment to induce peripheral inflammation and damage BBB, ultimately leading to neuroinflammation and synapse impairment.

However, certain limitations must be acknowledged. First, given that the sex of mice has been found to influence the progression of AD, with female mice being particularly susceptible due to variations in their physiological cycles and hormone levels [77], only male APP/PS1 mice was used to explore the influence of periodontitis on AD progression in the present study. A more in-depth investigation is needed to elucidate the effects of periodontitis on different AD models, taking into account both strain and sex. Additionally, the exact mechanisms by which periodontitis affects intestinal homeostasis, and how impaired intestinal homeostasis contributes to AD progression, remain to be fully elucidated.

Conclusions.

Within the limitations of this study, it was demonstrated that the disruption of intestinal homeostasis played a crucial role in the exacerbation of AD by periodontitis in APP/PS1 mice. Periodontitis could cause gut microbial dysbiosis, intestinal inflammation and

intestinal barrier impairment to induce peripheral inflammation and damage BBB, ultimately lead to neuroinflammation and synapse impairment. Remarkable alterations in the gut microbiota, such as *Lactobacillus* and *Anaerostipes*, were also noted during AD aggravation, suggesting their role as potential targets for preventing and managing AD. The present study proposes a novel perspective on the effect of periodontitis on AD and underscore the significance of the gut microbiota in elucidating the connection between periodontal infection and AD.

Supplementary Information

The online version contains supplementary material available at <https://doi.org/10.1186/s12974-024-03256-8>.

Supplementary Material 1

Acknowledgements

We thank Dr. Linying Zhou and Dr. Xi Lin (Electron Microscopy Lab of Public Technology Service Center, Fujian Medical University) for kindly providing technical assistance in electron microscopy.

Author contributions

XQ and KL designed the experiments and wrote the manuscript. XQ, XL, WH executed histological analysis and image acquisition. LZ executed signal quantification and statistical analyses. WC was involved in the construction of ligature model in mice. SG and SZ contributed to the writing and revision of the paper. XX and KL coordinated the research, supervised the data analysis, and revised the manuscript.

Funding statement

This work was supported by the National Natural Science Foundation of China (81860197, 82301103), the Joint Funds for the Innovation of Science and Technology, Fujian Province (2020Y9032) and the Educational Research Project for Young and Middle-aged Teachers of Fujian Provincial Department of Education (JAT220078).

Data availability

No datasets were generated or analysed during the current study.

Declarations

Ethics approval and consent to participate

All animal operations were performed following the protocol approved by the Animal Ethics Committee of Fujian Medical University (IACUC FJMU 2023-0035).

Consent for publication

Not applicable.

Competing interests

The authors declare no competing interests.

Conflict of interest

The authors assert that they possess no conflicts of interest.

Received: 12 August 2024 / Accepted: 7 October 2024

Published online: 18 October 2024

References

1. Slots J. Periodontitis: facts, fallacies and the future. *Periodontol* 2000. 2017;75:7–23.

2. Jepsen S, Suvan J, Deschner J. The association of periodontal diseases with metabolic syndrome and obesity. *Periodontol* 2000. 2020;83:125–53.
3. Sanz M, Marco Del Castillo A, Jepsen S, Gonzalez-Juanatey JR, D'Aiuto F, Boucharde P, et al. Periodontitis and cardiovascular diseases: Consensus report. *J Clin Periodontol*. 2020;47:268–88.
4. Lalla E, Papapanou PN. Diabetes mellitus and periodontitis: a tale of two common interrelated diseases. *Nat Rev Endocrinol*. 2011;7:738–48.
5. Carballo Á, López-Dequid I, Custodia A, Botelho J, Aramburu-Núñez M, Machado V, et al. Association of periodontitis with cognitive decline and its progression: contribution of blood-based biomarkers of Alzheimer's disease to this relationship. *J Clin Periodontol*. 2023;50:1444–54.
6. Rubinstein T, Brickman AM, Cheng B, Burkett S, Park H, Annavajhala MK, et al. Periodontitis and brain magnetic resonance imaging markers of Alzheimer's disease and cognitive aging. *Alzheimers Dement*. 2024;20:2191–208.
7. Dominy SS, Lynch C, Ermini F, Benedyk M, Marczyk A, Konradi A, et al. *Porphyromonas gingivalis* in Alzheimer's disease brains: evidence for disease causation and treatment with small-molecule inhibitors. *Sci Adv*. 2019;5:u3333.
8. Ryder MI, Xenoudi P. Alzheimer disease and the periodontal patient: new insights, connections, and therapies. *Periodontol* 2000. 2021;87:32–42.
9. Chen CK, Wu YT, Chang YC. Association between chronic periodontitis and the risk of Alzheimer's disease: a retrospective, population-based, matched-cohort study. *Alzheimers Res Ther*. 2017;9:56.
10. How KY, Song KP, Chan KG. *Porphyromonas gingivalis*: an overview of Periodontopathic Pathogen below the Gum line. *Front Microbiol*. 2016;7:53.
11. Kamer AR, Pirraglia E, Tsui W, Rusinek H, Vallabhajosula S, Mosconi L, et al. Periodontal disease associates with higher brain amyloid load in normal elderly. *Neurobiol Aging*. 2015;36:627–33.
12. Poole S, Singhrao SK, Kesavalu L, Curtis MA, Crean S. Determining the Presence of Periodontopathic virulence factors in short-term Postmortem Alzheimer's Disease Brain tissue. *J Alzheimers Dis*. 2013;36:665–77.
13. Sparks SP, Steffen MJ, Smith C, Jicha G, Ebersole JL, Abner E, et al. Serum antibodies to periodontal pathogens are a risk factor for Alzheimer's disease. *Alzheimers Dement*. 2012;8:196–203.
14. Ding Y, Ren J, Yu H, Yu W, Zhou Y. *Porphyromonas gingivalis*, a periodontitis causing bacterium, induces memory impairment and age-dependent neuro-inflammation in mice. *Immun Ageing*. 2018;15:6.
15. Qian X, Zhang S, Duan L, Yang F, Zhang K, Yan F, et al. Periodontitis deteriorates cognitive function and impairs neurons and Glia in a mouse model of Alzheimer's Disease. *J Alzheimers Dis*. 2021;79:1785–800.
16. Li F, Ma C, Lei S, Pan Y, Lin L, Pan C, et al. Gingipains may be one of the key virulence factors of *Porphyromonas gingivalis* to impair cognition and enhance blood-brain barrier permeability: an animal study. *J Clin Periodontol*. 2024;51:818–39.
17. Gu Y, Wu Z, Zeng F, Jiang M, Teeling JL, Ni J, et al. Systemic exposure to Lipopolysaccharide from *Porphyromonas gingivalis* induces bone loss-correlated Alzheimer's Disease-Like pathologies in Middle-aged mice. *J Alzheimers Dis*. 2020;78:61–74.
18. Wu Z, Ni J, Liu Y, Teeling JL, Takayama F, Collcutt A, et al. Cathepsin B plays a critical role in inducing Alzheimer's disease-like phenotypes following chronic systemic exposure to lipopolysaccharide from *Porphyromonas gingivalis* in mice. *Brain Behav Immun*. 2017;65:350–61.
19. Wu Z, Huang S, Li T, Li N, Han D, Zhang B, et al. Gut microbiota from green tea polyphenol-dosed mice improves intestinal epithelial homeostasis and ameliorates experimental colitis. *Microbiome*. 2021;9:184.
20. Chen C, Liao J, Xia Y, Liu X, Jones R, Haran J, et al. Gut microbiota regulate Alzheimer's disease pathologies and cognitive disorders via PUFA-associated neuroinflammation. *Gut*. 2022;71:2233–52.
21. Lourenço T, Spencer SJ, Alm EJ, Colombo A. Defining the gut microbiota in individuals with periodontal diseases: an exploratory study. *J Oral Microbiol*. 2018;10:1487741.
22. Lu J, Zhang S, Huang Y, Qian J, Tan B, Qian X, et al. Periodontitis-related salivary microbiota aggravates Alzheimer's disease via gut-brain axis crosstalk. *Gut Microbes*. 2022;14:2126272.
23. Qian J, Lu J, Cheng S, Zou X, Tao Q, Wang M, et al. Periodontitis salivary microbiota exacerbates colitis-induced anxiety-like behavior via gut microbiota. *Npj Biofilms Microbiomes*. 2023;9:93.
24. Xue L, Zou X, Yang XQ, Peng F, Yu DK, Du JR. Chronic periodontitis induces microbiota-gut-brain axis disorders and cognitive impairment in mice. *Exp Neurol*. 2020;326:113176.
25. Li L, Bao J, Chang Y, Wang M, Chen B, Yan F. Gut microbiota may mediate the influence of Periodontitis on prediabetes. *J Dent Res*. 2021;100:1387–96.
26. Huang Y, Liao Y, Luo B, Li L, Zhang Y, Yan F. Non-surgical Periodontal Treatment restored the gut microbiota and intestinal barrier in apolipoprotein E(-/-) mice with Periodontitis. *Front Cell Infect Mi*. 2020;10:498.
27. Wu XX, Huang XL, Chen RR, Li T, Ye HJ, Xie W, et al. Paenibacillus prevents intestinal barrier disruption and inhibits lipopolysaccharide (LPS)-induced inflammation in Caco-2 cell monolayers. *Inflammation*. 2019;42:2215–25.
28. Shin NR, Whon TW, Bae JW. Proteobacteria: microbial signature of dysbiosis in gut microbiota. *Trends Biotechnol*. 2015;33:496–503.
29. Rezai AR, D'Haese PF, Finomore V, Carpenter J, Ranjan M, Wilhelmsen K, et al. Ultrasound blood-brain barrier opening and Aducanumab in Alzheimer's Disease. *N Engl J Med*. 2024;390:55–62.
30. Wang Q, Huang X, Su Y, Yin G, Wang S, Yu B, et al. Activation of Wnt/ β -catenin pathway mitigates blood-brain barrier dysfunction in Alzheimer's disease. *Brain*. 2022;145:4474–88.
31. Zhong G, Long H, Zhou T, Liu Y, Zhao J, Han J, et al. Blood-brain barrier permeable nanoparticles for Alzheimer's disease treatment by selective mitophagy of microglia. *Biomaterials*. 2022;288:121690.
32. Tang Z, Liang D, Cheng M, Su X, Liu R, Zhang Y, et al. Effects of *Porphyromonas gingivalis* and its underlying mechanisms on Alzheimer-Like Tau Hyperphosphorylation in Sprague-Dawley Rats. *J Mol Neurosci*. 2021;71:89–100.
33. Kantarci A, Tognoni CM, Yaghmoor W, Marghalani A, Stephens D, Ahn JY, et al. Microglial response to experimental periodontitis in a murine model of Alzheimer's disease. *Sci Rep*. 2020;10:18561.
34. Suárez LJ, Arboleda S, Angelov N, Arce RM. Oral Versus Gastrointestinal Mucosal Immune niches in Homeostasis and Allostasis. *Front Immunol*. 2021;12:705206.
35. Koliarakis I, Messaritakis I, Nikolouzakis TK, Hamilos G, Souglakos J, Tsiaoussis J. Oral Bacteria and intestinal dysbiosis in Colorectal Cancer. *Int J Mol Sci*. 2019;20.
36. Erkert L, Gamez-Belmonte R, Kabisch M, Schödel L, Patankar JV, Gonzalez-Acera M, et al. Alzheimer's disease-related presenilins are key to intestinal epithelial cell function and gut immune homeostasis. *Gut*. 2024;10:1618–31.
37. Drummond E, Wisniewski T. Alzheimer's disease: experimental models and reality. *Acta Neuropathol*. 2017;133:155–75.
38. Aso E, Lomoio S, López-González I, Joda L, Carmona M, Fernández-Yagüe N, et al. Amyloid generation and dysfunctional immunoproteasome activation with disease progression in animal model of familial Alzheimer's disease. *Brain Pathol*. 2012;22:636–53.
39. Bibari O, Lee S, Dickson TC, Mitew S, Vickers JC, Chuah MI. Denervation of the olfactory bulb leads to decreased A β plaque load in a transgenic mouse model of Alzheimer's disease. *Curr Alzheimer Res*. 2013;10:688–96.
40. Lachén-Montes M, González-Morales A, de Morentin XM, Pérez-Valderrama E, Ausín K, Zelaya MV, et al. An early dysregulation of FAK and MEK/ERK signaling pathways precedes the β -amyloid deposition in the olfactory bulb of APP/PS1 mouse model of Alzheimer's disease. *J Proteom*. 2016;148:149–58.
41. Jungbauer G, Stähli A, Zhu X, Auber AL, Sculean A, Eick S. Periodontal micro-organisms and Alzheimer disease - A causative relationship? *Periodontol* 2000. 2022;89:59–82.
42. Kapila YL. Oral health's inextricable connection to systemic health: special populations bring to bear multimodal relationships and factors connecting periodontal disease to systemic diseases and conditions. *Periodontol* 2000. 2021;87:11–6.
43. Borsom EM, Conn K, Keefe CR, Herman C, Orsini GM, Hirsch AH, et al. Predicting Neurodegenerative Disease using Prepathology Gut Microbiota Composition: a longitudinal study in mice modeling Alzheimer's Disease pathologies. *Microbiol Spectr*. 2023;11:e345822.
44. Obrenovich M. Leaky gut, leaky brain? *Microorganisms*. 2018;6:107.
45. Aburto MR, Cryan JF. Gastrointestinal and brain barriers: unlocking gates of communication across the microbiota-gut-brain axis. *Nat Rev Gastroenterol Hepatol*. 2024;21:222–47.
46. Li L, Wang M, Bao J, Wang N, Huang Y, He S, et al. Periodontitis may impair the homeostasis of systemic bone through regulation of gut microbiota in ApoE(-/-) mice. *J Clin Periodontol*. 2022;49:1304–19.
47. Feng YK, Wu QL, Peng YW, Liang FY, You HJ, Feng YW, et al. Oral P. gingivalis impairs gut permeability and mediates immune responses associated with neurodegeneration in LRRK2 R1441G mice. *J Neuroinflammation*. 2020;17:347.
48. Kato T, Yamazaki K, Nakajima M, Date Y, Kikuchi J, Hase K, et al. Oral administration of *Porphyromonas gingivalis* alters the gut microbiome and serum metabolome. *Msphere*. 2018;3:e00460-18.

49. Lin S, Zhang X, Zhu X, Jiao J, Wu Y, Li Y, et al. *Fusobacterium nucleatum* aggravates ulcerative colitis through promoting gut microbiota dysbiosis and dysmetabolism. *J Periodontol*. 2023;94:405–18.
50. Sugiyama N, Uehara O, Morikawa T, Paudel D, Ebata K, Hiraki D, et al. Gut flora alterations due to lipopolysaccharide derived from *Porphyromonas gingivalis*. *Odontology*. 2022;110:673–81.
51. Wu L, Han J, Nie JY, Deng T, Li C, Fang C, et al. Alterations and correlations of gut microbiota and fecal metabolome characteristics in experimental periodontitis rats. *Front Microbiol*. 2022;13:865191.
52. Zhou LJ, Lin WZ, Liu T, Chen BY, Meng XQ, Li YL, et al. Oral pathobionts promote MS-like symptoms in mice. *J Dent Res*. 2023;102:217–26.
53. Heravi FS, Naseri K, Hu H. Gut microbiota composition in patients with neurodegenerative disorders (Parkinson's and Alzheimer's) and healthy controls: a systematic review. *Nutrients*. 2023;15:4365.
54. Hung CC, Chang CC, Huang CW, Nouchi R, Cheng CH. Gut microbiota in patients with Alzheimer's disease spectrum: a systematic review and meta-analysis. *Aging*. 2022;14:477–96.
55. Ye X, Liu B, Bai Y, Cao Y, Lin S, Lyu L, et al. Genetic evidence strengthens the bidirectional connection between gut microbiota and periodontitis: insights from a two-sample mendelian randomization study. *J Transl Med*. 2023;21:674.
56. Chen H, Peng L, Wang Z, He Y, Zhang X. Exploring the causal relationship between periodontitis and gut microbiome: unveiling the oral-gut and gut-oral axes through bidirectional mendelian randomization. *J Clin Periodontol*. 2024;51:417–30.
57. Vogt NM, Kerby RL, Dill-McFarland KA, Harding SJ, Merluzzi AP, Johnson SC, et al. Gut microbiome alterations in Alzheimer's disease. *Sci Rep*. 2017;7:13537.
58. Yang J, Wang L, Liu H, Xu H, Liu F, Song H, et al. Dysregulation of Ruminococcaceae and Megamonas could be predictive markers for rapid progression of mild cognitive impairment. *Microb Pathog*. 2023;183:106272.
59. Zhuang Z, Shen L, Li W, Fu X, Zeng F, Gui L, et al. Gut microbiota is altered in patients with Alzheimer's Disease. *J Alzheimers Dis*. 2018;63:1337–46.
60. Liu J, Yang G, Huang H, Shi C, Gao X, Yang W, et al. Dendritic cells targeting lactobacillus plantarum strain NC8 with a surface-displayed single-chain variable fragment of CD11c induce an antigen-specific protective cellular immune response. *Infect Immun*. 2020;88:e00759-19.
61. Rice TA, Bielecka AA, Nguyen MT, Rosen CE, Song D, Sonnerl ND, et al. Interspecies commensal interactions have nonlinear impacts on host immunity. *Cell Host Microbe*. 2022;30:988–1002.
62. Zhou W, Yang T, Xu W, Huang Y, Ran L, Yan Y, et al. The polysaccharides from the fruits of *Lycium barbarum* L. confer anti-diabetic effect by regulating gut microbiota and intestinal barrier. *Carbohydr Polym*. 2022;291:119626.
63. Shi YT, He JM, Tong ZA, Qian YJ, Wang QW, Jia D, et al. Ligature-Induced Periodontitis drives colorectal Cancer: an experimental model in mice. *J Dent Res*. 2023;102:689–98.
64. Gong S, Yan Z, Liu Z, Niu M, Fang H, Li N, et al. Intestinal microbiota mediates the susceptibility to Polymicrobial Sepsis-Induced Liver Injury by Granisetron Generation in mice. *Hepatology*. 2019;69:1751–67.
65. Zeng SL, Li SZ, Xiao PT, Cai YY, Chu C, Chen BZ, et al. Citrus polymethoxyflavones attenuate metabolic syndrome by regulating gut microbiome and amino acid metabolism. *Sci Adv*. 2020;6:x6208.
66. Kumaree KK, Prasanth MI, Sivamaruthi BS, Kesika P, Tencomnao T, Chaiyasut C, et al. *Lactobacillus paracasei* H101 enhances lifespan and promotes neuroprotection in *Caenorhabditis elegans*. *Sci Rep*. 2023;13:16707.
67. Kwon H, Lee EH, Park SY, Park JY, Hong JH, Kim EK, et al. *Lactobacillus*-derived extracellular vesicles counteract A β 42-induced abnormal transcriptional changes through the upregulation of MeCP2 and Sirt1 and improve A β pathology in Tg-APP/PS1 mice. *Exp Mol Med*. 2023;55:2067–82.
68. Bui T, Mannerås-Holm L, Puschmann R, Wu H, Troise AD, Nijse B, et al. Conversion of dietary inositol into propionate and acetate by commensal *Anaerostipes* associates with host health. *Nat Commun*. 2021;12:4798.
69. Salli K, Lehtinen MJ, Tiihonen K, Ouweland AC. Xylitol's health benefits beyond dental health: a comprehensive review. *Nutrients*. 2019;11:1813.
70. Nagpal R, Neth BJ, Wang S, Craft S, Yadav H. Modified Mediterranean-ketogenic diet modulates gut microbiome and short-chain fatty acids in association with Alzheimer's disease markers in subjects with mild cognitive impairment. *Ebiomedicine*. 2019;47:529–42.
71. Doifode T, Giridharan VV, Generoso JS, Bhatti G, Collodel A, Schulz PE, et al. The impact of the microbiota-gut-brain axis on Alzheimer's disease pathophysiology. *Pharmacol Res*. 2021;164:105314.
72. Sochocka M, Donskow-Lysoniewska K, Diniz BS, Kurpas D, Brzozowska E, Leszek J. The gut microbiome alterations and inflammation-driven pathogenesis of Alzheimer's Disease—a critical review. *Mol Neurobiol*. 2019;56:1841–51.
73. Fine N, Chadwick JW, Sun C, Parbhakar KK, Khoury N, Barbour A, et al. Periodontal inflammation primes the systemic Innate Immune Response. *J Dent Res*. 2021;100:318–25.
74. Bao J, Li L, Zhang Y, Wang M, Chen F, Ge S, et al. Periodontitis may induce gut microbiota dysbiosis via salivary microbiota. *Int J Oral Sci*. 2022;14:32.
75. Kitamoto S, Nagao-Kitamoto H, Jiao Y, Gilliland MR, Hayashi A, Imai J, et al. The intermucosal connection between the Mouth and Gut in Commensal Pathobiont-Driven colitis. *Cell*. 2020;182:447–62.
76. Gao C, Jiang J, Tan Y, Chen S. Microglia in neurodegenerative diseases: mechanism and potential therapeutic targets. *Signal Transduct Target Ther*. 2023;8:359.
77. Chen H, Liao Y, Zhang X, Shen H, Shang D, He Z, et al. Age- and sex-related differences of periodontal bone resorption, cognitive function, and immune state in APP/PS1 murine model of Alzheimer's disease. *J Neuroinflammation*. 2023;20:153.

Publisher's note

Springer Nature remains neutral with regard to jurisdictional claims in published maps and institutional affiliations.